iScience

CellPress
OPEN ACCESS

Article

Cell clusters containing intestinal stem cells line, the zebrafish intestine intervillus pocket

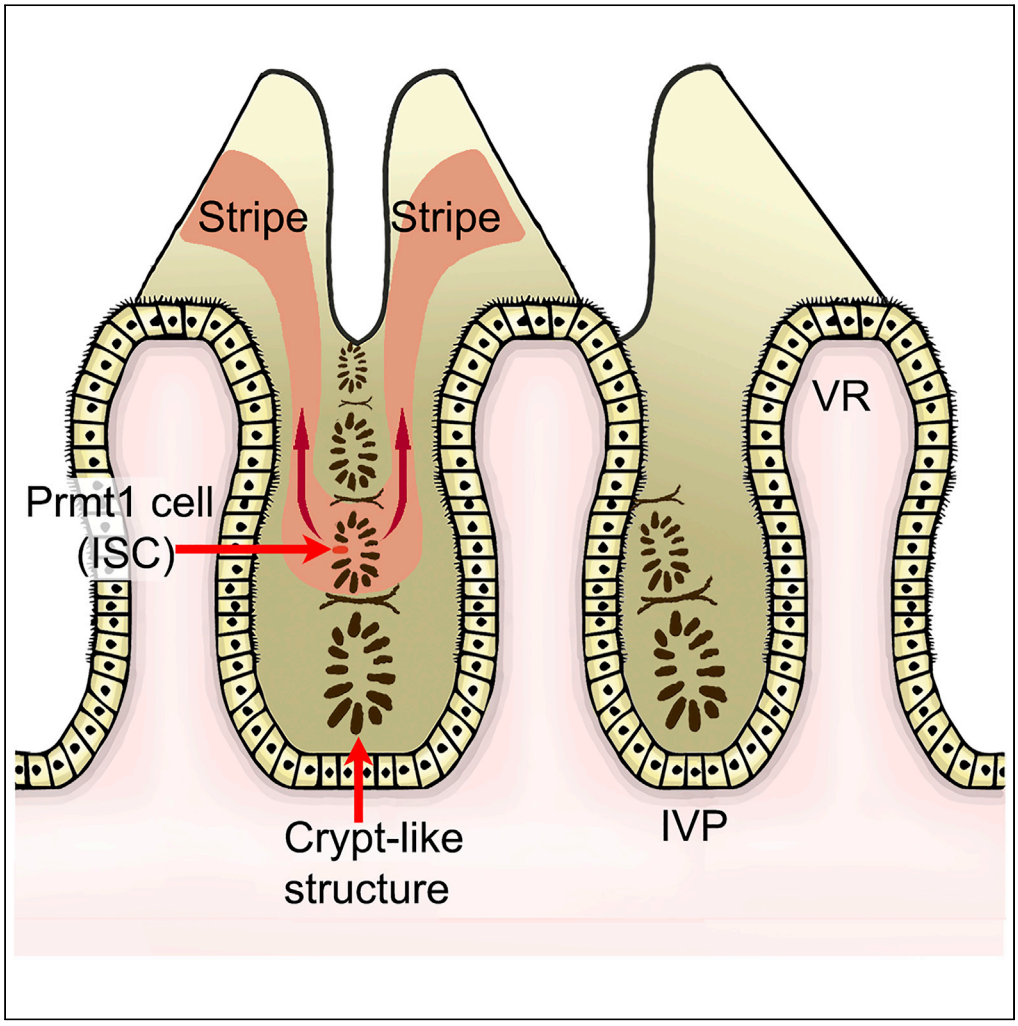

Sahar Tavakoli,
Shiwen Zhu, Paul
Matsudaira

sahartavakoli@fas.harvard.edu

Highlights

Prmt1 is an intestinal stem cell marker in zebrafish

Zebrafish intestinal stem cells reside within cell clusters lining the intervillus pocket

Stripes of newly reproduced epithelial cells originate from the cell clusters

Tavakoli et al., iScience *25*, 104280
May 20, 2022
https://doi.org/10.1016/j.isci.2022.104280

iScience

CellPress
OPEN ACCESS

Article

Cell clusters containing intestinal stem cells line, the zebrafish intestine intervillus pocket

Sahar Tavakoli,[1,2,3,*] Shiwen Zhu,[1] and Paul Matsudaira[1]

SUMMARY

In the mammalian intestine, stem cells (ISCs) replicate in basal crypts, translocate along the villus, and undergo cell death. This pattern of renewal occurs in the zebrafish intestine in which villi are elongated into villar ridges (VR) separated by intervillus pockets (IVP) but lack the infolded crypts. To understand how epithelial dynamics is maintained without crypts, we investigated the origin of epithelial lineage patterns derived from ISCs in the IVP of chimeric and zebrabow recombinant intestines. We found that the VR epithelium and IVP express the same recombinant colors when expression is under the control of ISC marker promoter *prmt1*. The expression originates from cell clusters that line the IVP and contain epithelial cells including Prmt1-labeled cells. Our data suggest that Prmt1 is a zebrafish ISC marker and the ISCs reside within basal cell clusters that are functionally analogous to crypts.

INTRODUCTION

In mice and human, the folded absorptive surface of the intestinal epithelium renews every two to five days (Leblond and Messier, 1958; Creamer et al., 1961) with newly replicated cells in basal crypts translocating apically to the villar tips (Krndija et al., 2019; Barker et al., 2008; Schmidt et al., 1985). This conveyor-belt-like process is maintained by intestinal stem cells (ISCs) (Cheng and Leblond, 1974), characterized by markers including LGR5 (Barker and Clevers, 2007), BMI1 (Sangiorgi and Capecchi, 2008), and LRIG1 (Powell et al., 2012), located in the crypts which provide a microenvironment for stem cell activity, interact tightly with the ISCs to regulate the fate of newly reproduced cells, and regulate rapid turnover of the intestinal epithelium (Sangiorgi and Capecchi, 2008; Clevers, 2013; Sakamori et al., 2012). A similar timing and pattern of epithelial renewal is exhibited in the less advanced architecture of the zebrafish and medaka intestine where the epithelium is folded into villar ridges (VRs) separated by valley-like intervillus pockets (IVPs) but are absent of crypts (Wallace et al., 2005; Pack et al., 1996). The absence of crypts in the zebrafish intestine raised the question of where the ISCs are located, whereas the ridge-shaped villi challenged the conventional pattern of intestinal epithelia renewal in zebrafish. Although it has been shown that the zebrafish intestinal epithelial progenitor cells are located at the intervillus pockets (IVPs) and the old differentiated cells shed off at the tip of the villus (Wallace et al., 2005; Crosnier et al., 2006; Wang et al., 2010; Li et al., 2020), the knowledge of zebrafish ISCs localization, intestinal epithelial regeneration pattern, and duration is still lacking.

To address these challenges, in this study, we first investigated the zebrafish intestinal epithelium duration with EdU label retention assay and created a chimera and recombinant of intestinal tissues to establish the epithelial renewal pattern in zebrafish intestine. Next, based on the previous literature we picked a list of candidate intestinal stem cell markers, screened the zebrafish genome for candidates' homolog and selected *prmt1* for further analysis. *Prmt1* gene encodes protein arginine N-methyltransferase 1, which plays an important role by transferring methyl groups during post-translational modification of target proteins (Zhang and Cheng, 2003). Using lineage tracing experiments and antibody staining, we confirmed that Prmt1-expressing cells display characteristics of the adult stem cells and are responsible for epithelia renewal of the zebrafish intestine. Using high resolution imaging, we traced the multi-colored pattern of epithelial renewal in Zebrabow recombinant intestinal tissues upon tamoxifen activation under control of *prmt1* promoter. The zebrabow expression not only produced stripes that flank an IVP but surprisingly the stripes are continuous with clusters of cells that line the base of the IVP. These results suggest that Prmt1 is an ISC marker in zebrafish and reveal, for the first time, that cells lining the base of the zebrafish IVPs are arranged in discrete cell clusters, which function as crypts in renewing the flanking VR epithelium.

[1]Center for BioImaging Sciences, Department of Biological Sciences, Mechanobiology Institute, National University of Singapore, Singapore 119077, Singapore

[2]Present address: Harvard Department of Stem Cell and Regenerative Biology, Cambridge, MA 02138, USA

[3]Lead contact

*Correspondence: sahartavakoli@fas.harvard.edu

https://doi.org/10.1016/j.isci.2022.104280

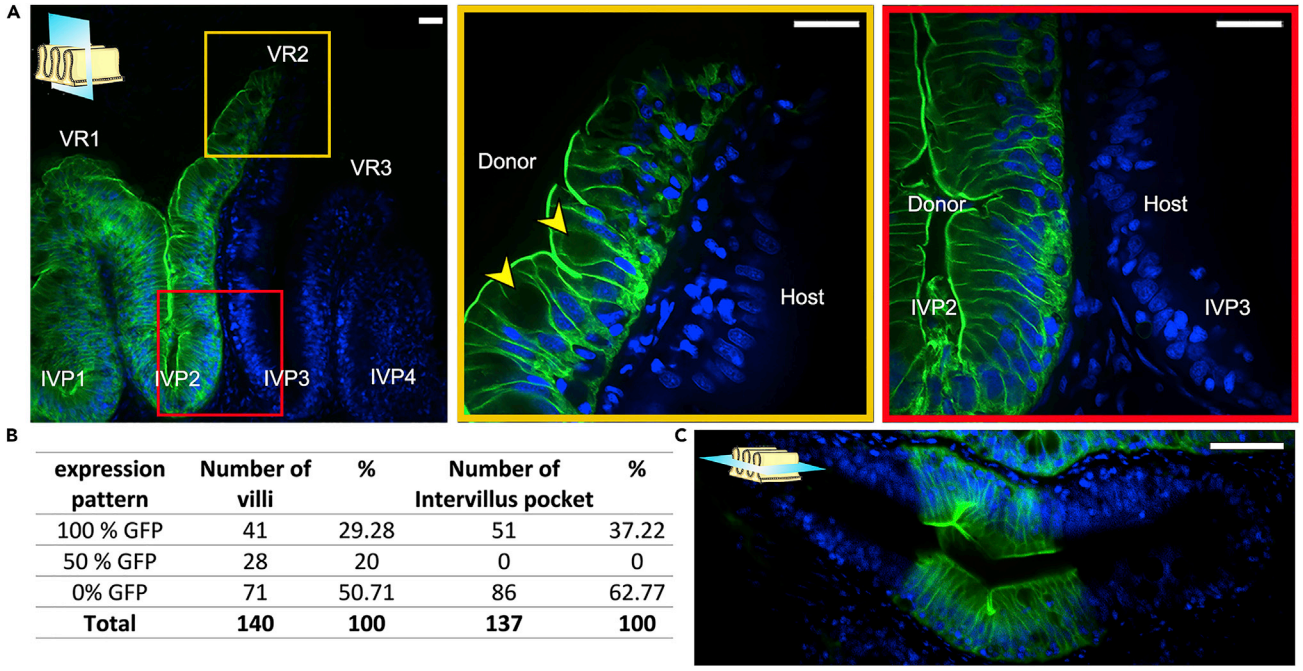

expression pattern	Number of villi	%	Number of Intervillus pocket	%
100 % GFP	41	29.28	51	37.22
50 % GFP	28	20	0	0
0% GFP	71	50.71	86	62.77
Total	**140**	**100**	**137**	**100**

Figure 1. Regeneration in chimeric intestine IVP and VR

(A) Chimeric tissue includes the host- (blue) and donor- (green) derived cells. Left Panel: Donor-derived IVP1, IVP2, VR1, host-derived IVP3, IVP4, VR3, and chimeric VR2 (yellow box). Middle panel: Enlarged image of VR2 (yellow box) showing mGFP-labeled epithelia. mGFP originates from the transplanted blastomere cells and expressed by epithelial cells including goblet cells (yellow arrowheads) and enterocytes. Right panel: Higher magnification of VR2 and the flanking IVP2 and IVP3 (red box). Nuclei labeled with DAPI (blue) and cell membrane labeled with mGFP (green). Scale bar = 40 μm.

(B) Quantitation of GFP expression in villi and intervillus pockets. 100% GFP: mGFP expression pattern has been detected at both sides of the intestinal villus or IVP, 50% GFP: Examples where only one side expresses mGFP. 0% GFP: Absence of mGFP expressing epithelia (n = 140).

(C) Transverse Z-section midway through two facing and chimeric VRs' tip. The two facing VRs share an intervening IVP and have a mirrored phenotype. Nuclei labeled with DAPI (blue) and cell membrane labeled with mGFP (green). Panel B shows the n for this experiment. Scale bar = 40 μm. All the tissue samples were from anterior and middle sections of the zebrafish intestine.

RESULTS

Epithelial cells translocate from IVP to VR in 48 hours

Previous works have established that intestinal epithelia in the zebrafish translocates from the intervillous pocket (Matsuda and Shi, 2010; Aghaallaei et al., 2016; Wallace et al., 2005; Crosnier et al., 2005; Wang et al., 2010) but the translocation time varies from 2–7 days among various reports (Wallace et al., 2005; Aghaallaei et al., 2016). One reason for the variation could be differences in villar ridge height. Thus, we reinvestigated the renewal pattern by labeling the proliferating cells with continuous pulses of EdU oral administration. The intestinal epithelium in adult fish was exposed to EdU molecules every 12 h. In VRs that were 350–450 μm-tall, the EdU incorporated into replicating cells in the IVP and by 48 h the labeled cells reached the tips (Figures S1A–S1C). The two-day translocation time is comparable to the transit time measured in the zebrafish and mouse intestine (Wallace et al., 2005; Crosnier et al., 2005; Krndija et al., 2019; Creamer et al., 1961; Aghaallaei et al., 2016) and corresponds to an average translocation velocity of 8 μm/h.

If replication originates in the IVP (Figure S1B, 0.5 hpt and Figure S1B and S1C, 12 hpt), then it is reasonable to assume that dividing cells including transit amplifying cells (TACs) and ISCs are located in the IVP (Wallace et al., 2005; Faro et al., 2009; Li et al., 2020). We could confirm the presence of progenitor cells including ISCs through blastomere cell transplantation: 25 membrane-bound mGFP (*β-actin:mGFP*) donor blastomere cells were transplanted from the area of the presumptive intestine in the yolk sac margin (Warga and Nusslein-Volhard, 1999) into analogous positions in unlabeled AB host embryos. We tracked the renewal of chimeric intestines 3–5 months post transplantation, at the adult stage. From 140 longitudinal sections of adult intestines, we observed VRs that were either labeled, half labeled (chimeric), or unlabeled (Figures 1A left and middle panel and 1B). In comparison, IVPs were either labeled or unlabeled but

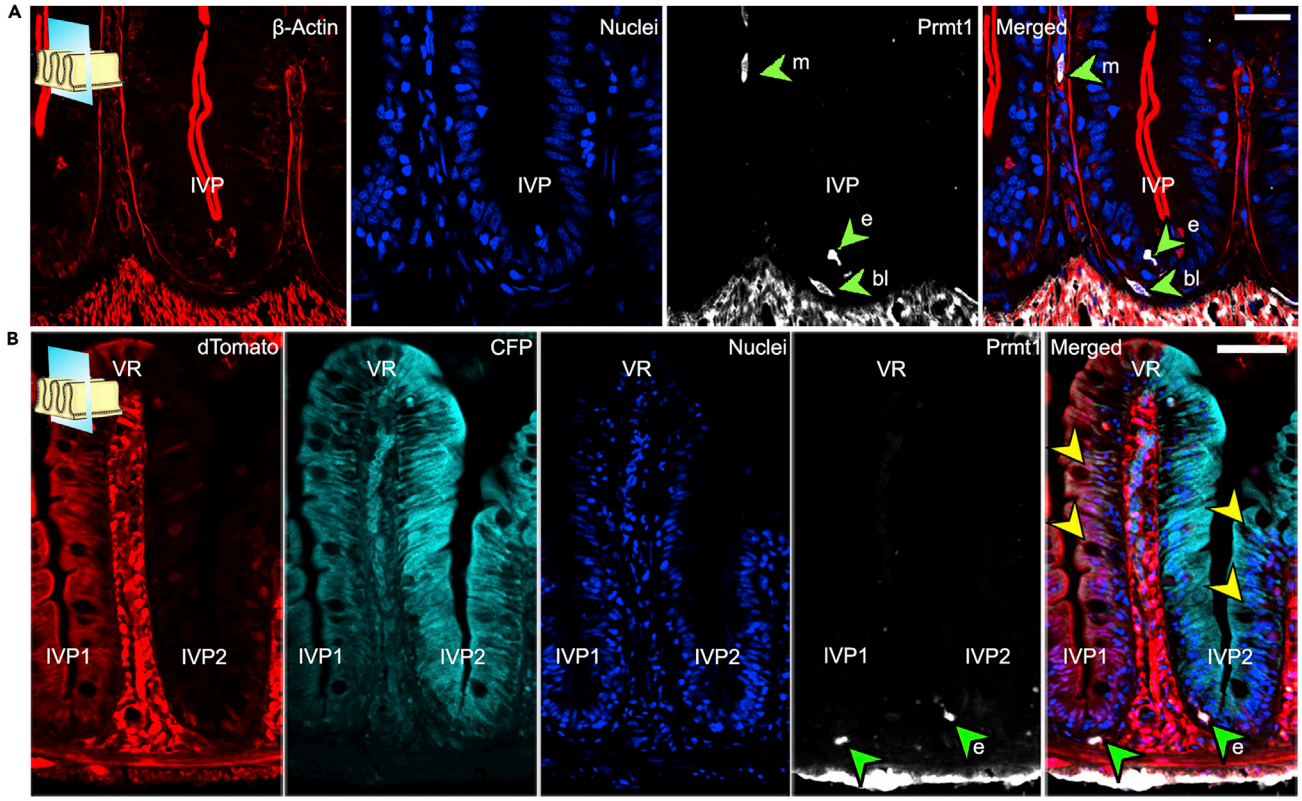

Figure 2. Localization of Prmt1-expressing cells in the intervillous pocket

(A) Longitudinal sections of an adult zebrafish intestine stained with anti-β-actin antibody (red), DAPI (blue) and anti-PRMT1 antibody (white). Prmt1 expression is localized within the mesenchyme (arrowhead m), adjacent to the basal lamina (arrowhead bl), or within the basal epithelium (arrowhead e). n > 10. Scale bar = 40 μm.

(B) Longitudinal sections of promoter-driven recombinant tissues and stained with anti-PRMT1 antibody (white). $CreER^{T2}$ under control of the *prmt1* promoter changes the dTomato (red) expression to CFP (cyan) expression in enterocytes and goblet cells (yellow arrowheads) lining the flanking walls of IVP2. Anti-PRMT1 labeled cells (white) are located at the base of IVP1 and IVP2 (green arrowheads). Nuclei are labeled with DAPI (blue). n > 10. Scale bar = 40 μm. All the tissue samples were from anterior and middle sections of the zebrafish intestine.

not half labeled (Figures 1A left and right panel and 1B). Figure 1C shows transverse Z-section midway through two facing VRs, which are GFP positive (differentiated from donor progenitors) in the middle and GFP negative (differentiated from host progenitors) at the either ends. This pattern results in a 1IVP:2VR ratio in which, the faces of the flanking VRs share the same label as the nearest IVP and is best explained by ISCs located in the IVP and renewing the faces of the flanking VRs (Figures 1A–1C). Tracking the GFP-positive epithelium at the adult stage, while the GFP-positive cells were transplanted at the blastula stage, reveals the presence of the donor blastomere-derived ISCs in the recipient intestine.

Prmt1-expressing cells renew the zebrafish intestinal epithelium

Based on the evidence for ISCs in IVPs from the chimera experiments, we searched the zebrafish genome for homologs of mouse and human ISC marker (Matsuda and Shi, 2010; Powell et al., 2012; Sangiorgi and Capecchi, 2008) and selected *prmt1* for further analysis (Figure S2). Prmt1 has been reported in model organisms such as *C. elegans* (Zhang and Cheng, 2003), identified as ISCs marker in frogs, and is also detected in zebrafish intestine IVP (Matsuda and Shi, 2010; Ishizuya-Oka and Shi, 2011). We probed for Prmt1-expressing cells by immunofluorescence with anti-PRMT1 antibody. In longitudinal sections, the antibody detected small round cells (white) in the epithelium at or near the base of an IVP (green arrowheads), adjacent to the underlying basal lamina (Figure 2). In other sections, the antibody detects Prmt1-expressing cells not only in the IVP epithelium (Figure 2A, arrowhead e) but also in the basal lamina of a VR (Figure 2A, arrowhead bl) and in the mesenchyme subjacent to the basal lamina bordering an IVP (Figure 2A, arrowhead m). Figure S3, confirms the presence of Prmt1-expressing cells using lineage tracing

experiment in the *Tg* (*prmt1*:*mCherry-CreER*^{T2}). The Prmt1-expressing cells are scattered in the intestinal epithelium, mesenchyme, and basal lamina. Thus, 12 μm thick longitudinal sections of the zebrafish intestine may not contain all 3 different types of Prmt1-expressing cells (Figure 2B).

The presence of chimeric VRs but absence of chimeric IVPs in the embryo transplantation experiments can be tested in recombinant lineage tracing experiments to investigate directly whether Prmt1 is an ISC marker. Zebrabow is a powerful lineage tracing to assess the clonality in a tissue using multicolor fluorophore cassette (Pan et al., 2013). A nonrecombinant Zebrabow Intestinal tissue expresses dTomato, while the activation of CreER^{T2} under an ISC promoter edits the cassette to express either CFP or YFP. Thus, we imaged the multi-color Zebrabow intestine 4 days (Figure S4A) and 2 weeks (Figures 2B and S4B) after tamoxifen activation of *prmt1* promoter-dependent Cre-recombinase enzymes in *Tg* (*ubi*:*Zebrabow*;*prmt1*:*mCherry-CreER*^{T2}) double transgenic lines. Consistent with the ratio of labeled structures found in the transplanted chimeric intestines (Figures 1A–1C), we observed the same 1IVP:2VR pattern of zebrabow recombination under the control of the *prmt1* promoter (Figures 2B and S4A). Shortly after CreER^{T2} activation, the newly reproduced cells, which are originated from a recombinant Prmt1 cells, translocate halfway toward the VR tip (Figure S4A), while 2 weeks after CreER^{T2} activation, the longitudinal (Figure 2B) and *en face* (Figure S4B) view of VRs show the recombinant stripes reached the VR tip. Furthermore, the entire differentiated epithelium including goblet cells (Figure 2B, yellow arrowheads) as well as enterocytes displayed the same recombinant color of the nearest IVP. Thus, the multi-color expression from the *prmt1*-promoter not only originates from cells in the IVP but also these cells renew the differentiated cells of the villus epithelium. Our results suggest that Prmt1 is a marker for zebrafish ISCs and these ISCs are located in the IVP.

Next, we tested whether villus architecture is altered by inhibiting the expression of *prmt1* with its corresponding Vivo-Morpholinos (MO) (Tsai et al., 2011). After gavaging MOs into the gut, we imaged longitudinal sections of treated and untreated intestines. The images showed reduced VR heights of prmt1-MO-treated intestines (Figures S5C and S5D) compared to the un-injected (Figure S5A) or control MO-treated (Figure S5B) intestines as negative control. Reduced VR heights were also observed in our positive control treated with the known ISCs' marker morpholino: bmi1a-MO and lrig1-MO (Figures S5E and S5F). Shortened VRs are the expected effect for genes with an ISC role and suggest that Prmt1 is an ISC marker.

ISCs reside within cell clusters lining the intervillus pocket

To understand how ISCs in the IVP regenerate the flanking VRs requires a more detailed investigation of the IVP structure. While in longitudinal views of the zebrafish intestine, an IVP is a continuous U-shaped epithelium (Figures 1A, 2A, and 2B), the organization of the epithelium along the length of an IVP and the location of ISCs in the IVP are unknown. Thus, we reconstructed in 3D a portion of a *prmt1* induced Zebrabow recombinant intestine consisting of an IVP flanked by a pair of VRs (Figure 3A and Video S1). Transverse Z-sections midway through a VR (Figure 3A, left column and Video S1) show the recombinant color expressed by the flanking VR epithelium (VR1/VR2) is also expressed by the intervening IVP (IVP1). In addition to the epithelium, the mesenchyme of the lamina propria extends from the core of the VR (Figure 2B) basally and wraps around to underlie the IVP epithelium (Figure 3A).

Surprisingly, in a plan view along an IVP, the epithelium is not continuous but is organized into ellipsoidal clusters of radially arranged cells: IVP1a, IVP1b (recombinant) and IVP1c (nonrecombinant) (Figure 3A, columns 2–4, Videos S1, and S2). A cluster is approximately 37 × 54 μm and bordered by mesenchyme of the VR lamina propria (Figures 3A, 3D–3G, Videos S1, and S2). Furthermore, anti-PRMT1 antibody (white) labels a single cell in each cell cluster (Figure 3A and Video S2, green arrowheads) and also additional cells associated with the mesenchyme. ISCs constitute a small proportion of epithelial cells (Barker et al., 2008; Sangiorgi and Capecchi, 2008; Aghaallaei et al., 2016; Leblond and Messier, 1958); Thus, there are not many Prmt1-labeled cells in the zebrafish intestinal epithelium. Interestingly, this radial arrangement of the cell cluster is strikingly similar to a cross-section through a mouse intestinal crypt embedded in the mesenchyme of the lamina propria (Figures 3D–3G) (Sumigray et al., 2018).

Stripes originate from the IVP cell clusters

The stripe of the VR epithelium from an IVP is similar to the classic pattern of epithelial stripes that originate from mouse crypts (Schmidt et al., 1985). Thus, if an IVP cell cluster is functionally analogous to a crypt, then

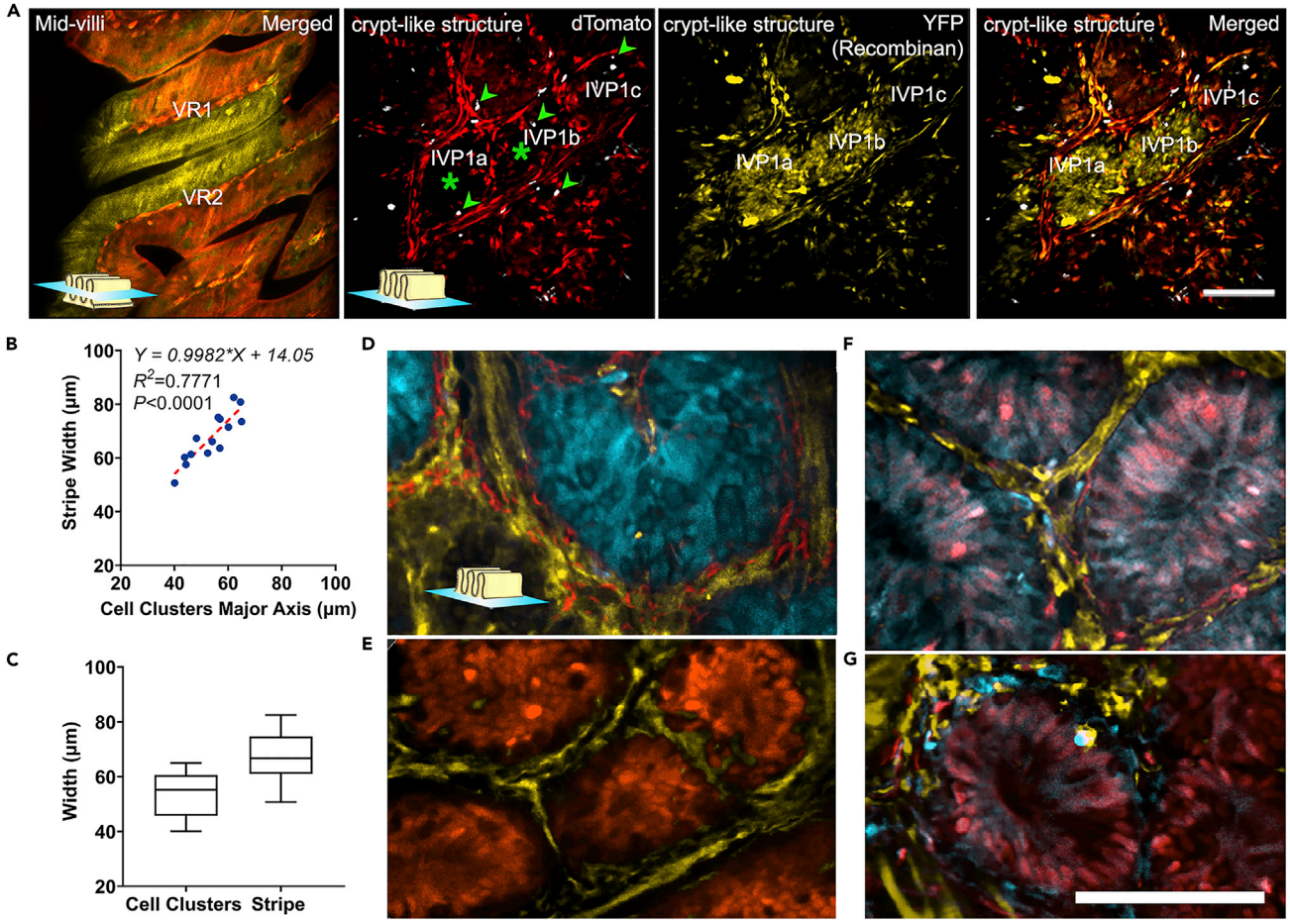

Figure 3. Ellipsoid cell clusters lining the IVP, are units of origin of villar epithelial renewal

(A) Transverse Z-sections of promoter-driven recombinant tissues, which is stained with anti-PRMT1 antibody (white). 12–15 nm thick x-y optical slices through the middle of VRs (left column) and base of an IVP of *ubi*:*Zebrabow* tissues expressing dTomato (red), YFP (yellow), or CFP (cyan) under the *prmt1* promoter from Video S1. Anti-Prmt1-labeled cells (white) are found in ellipsoidal cell clusters (green arrowheads) at the bottom of an IVP. Recombinant clusters (IVP1a and IVP1b) are indicated with green asterisks (*). n > 5. Scale bar = 40 µm.

(B) Stripe width is correlated with the cell cluster length: A plot of the major axis (x axis) of the ellipsoidal cell clusters in the IVP versus the width of the stripe at the base of the IVP (y axis). The slope, intercept, and regression analysis measure the correlation between cell cluster length and stripe width (n = 14).

(C) Box and whisker graph of cell clusters major axis and stripe width (n = 14), Data are represented as min to max, line at median.

(D and E) Bottom and (F and G) middle of cell clusters line in the zebrafish intervillous pocket. Non recombinant (left panel) and recombinant (right panel) IVP cell clusters from *Tg* (*ubi*:*Zebrabow*;*prmt1*:*mCherry-CreER*^{T2}) double transgenic fish are bordered by mesenchyme. dTomato (Red), YFP (Yellow), mCerulean (Blue). Scale bar = 40 µm. All the tissue samples were from anterior and middle sections of the zebrafish intestine.

there should be a direct relationship between the location and size of an IVP cluster and its flanking stripes. We measured the widths of recombinant VR stripes and the length of its corresponding cell cluster in the IVP (Figures 3B and 3C) and found a well-correlated (0.77) relationship between stripe and cluster in which stripe width, 67 ± 9 µm closely matches cluster length 54 ± 8 µm. The variation in the width of stripes and lengths of clusters is two cell diameters and is within the error of the measurement. This one-to-one correspondence in dimension and position is conclusive evidence that a cluster functions similar to a crypt, inhabits ISCs and forms a stripe.

DISCUSSION

Renewal of the intestinal epithelia is a continuous process, maintained by stem cells which differentiate into various epithelia cells that translocate from the base to the tip of the villus. Similar to mice and human where ISCs have been reported in intestinal crypts (Potten et al., 1982; Crosnier et al., 2005; Leblond

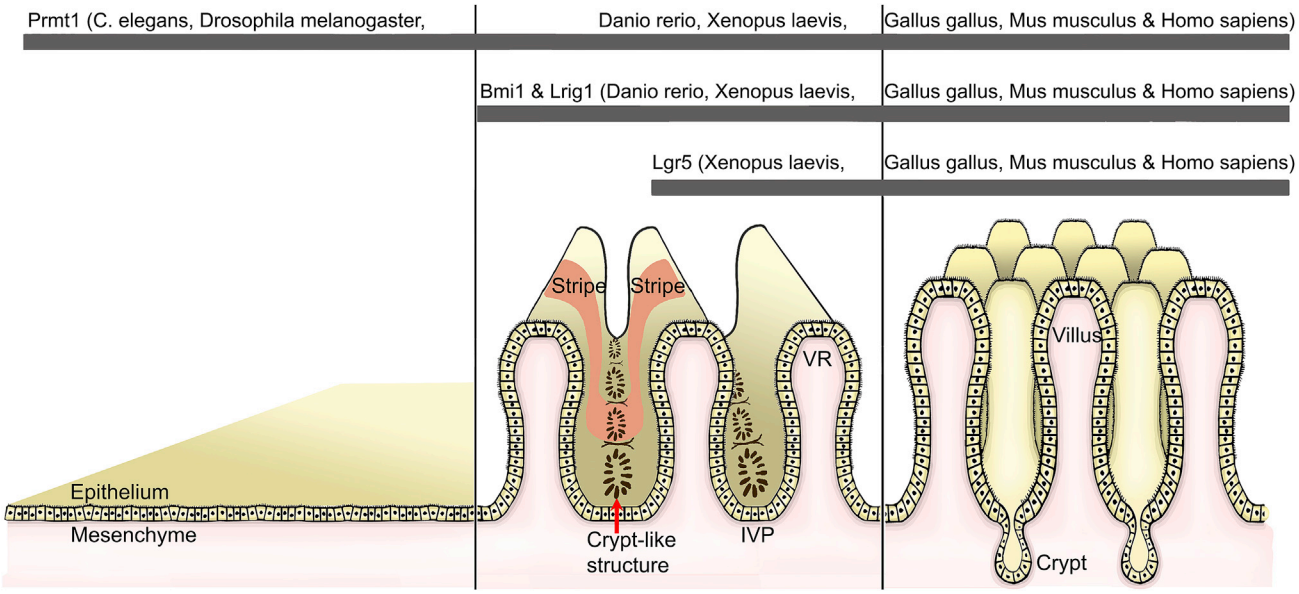

Figure 4. Comparison of intestinal surface architectures

The gastrointestinal tract is a simple tube in invertebrate model organisms *C. elegans* and *Drosophila melanogaster's* intestine but is folded into ridges and stereotypical paddle-shaped villi lining the surface of amphibia, zebrafish, avian, and mammalian intestines. In the zebrafish (middle column of schematic figure), stripes of epithelium on flanking villar ridges (VR) originate from ellipsoidal cell clusters that are aligned along the intervillous pocket (IVP). *Prmt1* is conserved as an intestinal stem cell marker located in the cell clusters.

and Messier, 1958; Krndija et al., 2019; Barker et al., 2008), zebrafish ISCs are located in the crypt-less intervillus pocket (IVP) (Peron et al., 2020). But, the origin of epithelial regeneration and translocation remained unexplored (Matsuda and Shi, 2010). In this study, we traced the lineage of intestinal epithelia renewal with high-resolution imaging and our results provided direct evidence of Prmt1 as a zebrafish ISC marker localized in crypt-like clusters of cells at the base of the IVP, from the which intestinal epithelia renewal originates.

Classic lineage tracing studies by Ponder and colleagues established that the mouse villar epithelium originates from the nearest crypts (Ponder et al., 1985; Schmidt et al., 1985). Because a single villus is surrounded by multiple crypts, the villus epithelium originates from different ISCs in surrounding crypts (Schmidt et al., 1985; Snippert et al., 2010). Similarly, our lineage tracing experiments demonstrate that the villar ridge is chimeric as a result of epithelial renewal originating from an IVP, consists of several cell clusters, and distributed bilaterally as a broad stripe along the flanking VRs. Although the zebrafish intestine lacks an invaginated crypt (Wallace et al., 2005), the 3D reconstruction documents that the valley-like IVP is compartmentalized into flat clusters of cells that function as crypts and share similarities in structure (Figure 4). The evidence that the cell clusters function as crypts are the following: First, ISCs reside in the clusters. For the zebrafish intestine our lineage tracing and antibody labeling results identify Prmt1 as an ISC marker. Zebrafish epithelial renewal is under control of Prmt1 and clearly linked to the IVP cluster (Figure S6). Because *CreER*^{T2} is expressed under the promoter of the intestinal stem cell marker gene (*prmt1*), upon tamoxifen activation, a permanent recombination will only happen in the intestinal stem cells (Prmt1-expressing cells). Thereafter, all the daughter cells carry the recombinant genotype and express the same phenotype as the recombinant Prmt1-stem cell (Figure S6, red and green arrowheads). Second, although the cell cluster is flat and not invaginated into a crypt, the radial arrangement of cells in a cluster has the appearance of a crypt in transverse cross-section; this morphology is similar to intervillar units in mice at postnatal day 0 and before crypt formation (Sumigray et al., 2018). Furthermore, a cluster is slightly smaller than the cross-section diameter of a mouse intestinal crypt (35–45 μm) (Martin et al., 1998). Third, crypts are finger-like invaginations of epithelium separated by mesenchymal tissue of the lamina propria and continuous with the mesenchyme of the villus (Sumigray et al., 2018). Similarly, the IVP cell clusters are separated by thin strands of mesenchyme which are continuous with the mesenchyme in the core of a villar ridge (Figures 2B, 3A, 3D, Videos S1 and S2).

These similarities between crypt and cell cluster are consistent with a cell cluster as the unit of origin of villar epithelial renewal.

The crypt-less organization of the mammalian intestine is a transient state in the postembryonic development of the mouse intestine and may reflect a stage in the evolution of the mammalian intestine. Our results suggest that the cell clusters in the VR/IVP architecture of zebrafish represent an intermediate step from the simple tubular architecture of worms and flies to the crypt/villus architecture of birds and mammals (Figure 4).

Limitations of the study

This study describes the substructure in the IVP in the form of a circular cluster of epithelial cells, similar to the view down a crypt. Furthermore, Prmt1-expressing cells were previously localized in the IVP of the zebrafish intestine by *in situ* hybridization (Matsuda and Shi, 2010) but not to a single cell. In our study, we not only extend the details of Prmt1-localization to a specific cell but also uncover the arrangement of cells in flattened cell clusters and demonstrate that the prmt1 promoter can drive a striped pattern of expression that replicates a stem cell-derived lineage as first described in mice (Potten et al., 1982). In addition, we used morpholino oligo containing the same sequence as used by Tsai et al. (2011) but were linked to a moiety that enhanced delivery across the membrane (Vivo-Morpholino, GeneTool). Although there are well-known artifacts associated with morpholino-experiments (limitation), we tested the intestinal stem cell marker gene (*prmt1*) using the previously evaluated sequence (Tsai et al., 2011) and reported experimental procedure reported by Matsuda and Shi for the Xenopus intestine (Matsuda and Shi, 2010). We observed the same results, but we did not investigate further as we were only confirming the prior work from other labs to justify our choice of possible ISC marker promoter. The promoter-driven Zebrabow expression was designed to confirm the identity of an ISC marker gene.

STAR★METHODS

Detailed methods are provided in the online version of this paper and include the following:

- KEY RESOURCES TABLE
- RESOURCE AVAILABILITY
  - Lead contact
  - Material availability
  - Data and code availability
- EXPERIMENTAL MODEL AND SUBJECT DETAILS
  - Fish and transgenic lines
  - Creation of chimera by cell transplantation
  - Generation of transgenic lines of zebrafish for lineage tracing
- METHOD DETAILS
  - *In vivo* labeling of proliferating intestinal epithelium cells with EdU
  - Morpholino oral administration
- QUANTIFICATION AND STATISTICAL ANALYSIS
- ADDITIONAL RESOURCES
  - Imaging
  - Confocal microscopy
  - Image processing and analysis

SUPPLEMENTAL INFORMATION

Supplemental information can be found online at https://doi.org/10.1016/j.isci.2022.104280.

ACKNOWLEDGMENTS

We thank the following individuals for contributing fish and constructs: V. Korzh (Institute of Molecular and Cell Biology (IMCB), Singapore) for providing the *Tg* (*β-actin:mGFP*) line, S. Hans (Dresden University of Technology, Germany) for providing the *Tg* (*hsp70L:mCherry-CreER*^{T2}) line, A. Pan and A. Schier (Harvard University, United States of America) for the *ubi:Zebrabow* fish, Z. Gong (National University of Singapore (NUS), Singapore) for the pMDS6 construct, N. Barker (IMCB, Singapore) for the CreER^{T2} construct. We thank Z. Gong, and C. Winkler (NUS) for their helpful comments and discussion. We also thank S. N.

Chan for critically reviewing the manuscript. This study was supported by Singapore International Graduate Award (SINGA), Mechanobiology Institute, Centre for BioImaging Sciences (CBIS) and NUS.

AUTHOR CONTRIBUTIONS

S.T. generated the chimeric zebrafish, *Tg* (*prmt1:mCherry-CreER*^{T2}) strain, carried out all the experiments, collected all the confocal images. S.T. and S.Z. processed and analyzed the image data. P.M. supervised the research. S.T. and P.M. planned the studies and wrote the manuscript. S.T., S.Z., S.N.C., and P.M. edited the manuscript.

DECLARATION OF INTERESTS

The authors declare no competing interests.

Received: August 4, 2021
Revised: December 12, 2021
Accepted: April 19, 2022
Published: May 20, 2022

REFERENCES

Aghaallaei, N., Gruhl, F., Schaefer, C.Q., Wernet, T., Weinhardt, V., Centanin, L., Loosli, F., Baumbach, T., and Wittbrodt, J. (2016). Identification, visualization and clonal analysis of intestinal stem cells in fish. Development *143*, 3470–3480. https://doi.org/10.1242/dev.134098.

Barker, N., and Clevers, H. (2007). Tracking down the stem cells of the intestine: strategies to identify adult stem cells. Gastroenterology *133*, 1755–1760. https://doi.org/10.1053/j.gastro.2007.10.029.

Barker, N., Van De Wetering, M., and Clevers, H. (2008). The intestinal stem cell. Genes Dev. *22*, 1856–1864.

Cheng, H., and Leblond, C.P. (1974). Origin, differentiation and renewal of the four main epithelial cell types in the mouse small intestine V. Unitarian theory of the origin of the four epithelial cell types. Am. J. Anat. *141*, 537–561. https://doi.org/10.1002/aja.1001410407.

Clevers, H. (2013). The intestinal crypt, a prototype stem cell compartment. Cell *154*, 274–284. https://doi.org/10.1016/j.cell.2013.07.004.

Creamer, B., Shorter, R.G., and Bamforth, J. (1961). The turnover and shedding of epithelial cells: Part I the turnover in the gastro-intestinal tract. Gut *2*, 110–116. https://doi.org/10.1136/gut.2.2.110.

Crosnier, C., Stamataki, D., and Lewis, J. (2006). Organizing cell renewal in the intestine: stem cells, signals and combinatorial control. Nat. Rev. Genet. *7*, 349–359. https://doi.org/10.1038/nrg1840.

Crosnier, C., Vargesson, N., Gschmeissner, S., Ariza-Mcnaughton, L., Morrison, A., and Lewis, J. (2005). Delta-Notch signalling controls commitment to a secretory fate in the zebrafish intestine. Development *132*, 1093–1104. https://doi.org/10.1242/dev.01644.

Erturk, A., Mauch, C.P., Hellal, F., Forstner, F., Keck, T., Becker, K., Jahrling, N., Steffens, H., Richter, M., Hübener, M., et al. (2012). Three-dimensional imaging of the unsectioned adult spinal cord to assess axon regeneration and glial responses after injury. Nat. Med. *18*, 166–171. https://doi.org/10.1038/nm.2600.

Faro, A., Boj, S.F., and Clevers, H. (2009). Fishing for intestinal cancer models: unraveling gastrointestinal homeostasis and tumorigenesis in zebrafish. Zebrafish *6*, 361–376. https://doi.org/10.1089/zeb.2009.0617.

Ishizuya-Oka, A., and Shi, Y.B. (2011). Evolutionary insights into postembryonic development of adult intestinal stem cells. Cell Biosci. *1*, 37. https://doi.org/10.1186/2045-3701-1-37.

Krndija, D., El Marjou, F., Guirao, B., Richon, S., Leroy, O., Bellaiche, Y., Hannezo, E., and Matic Vignjevic, D. (2019). Active cell migration is critical for steady-state epithelial turnover in the gut. Science *365*, 705–710. https://doi.org/10.1126/science.aau3429.

Leblond, C.P., and Messier, B. (1958). Renewal of chief cells and goblet cells in the small intestine as shown by radioautography after injection of thymidine-H3 into mice. Anat. Rec. *132*, 247–259. https://doi.org/10.1002/ar.1091320303.

Li, J., Prochaska, M., Maney, L., and Wallace, K.N. (2020). Development and organization of the zebrafish intestinal epithelial stem cell niche. Dev. Dyn. *249*, 76–87. https://doi.org/10.1002/dvdy.16.

Martin, K., Kirkwood, T.B.L., and Potten, C.S. (1998). Age changes in stem cells of murine small intestinal crypts. Exp. Cell Res. *241*, 316–323. https://doi.org/10.1006/excr.1998.4001.

Matsuda, H., and Shi, Y.B. (2010). An essential and evolutionarily conserved role of protein arginine methyltransferase 1 for adult intestinal stem cells during postembryonic development. Stem Cells *28*, 2073–2083. https://doi.org/10.1002/stem.529.

Pack, M., Solnica-Krezel, L., Malicki, J., Neuhauss, S.C., Schier, A.F., Stemple, D.L., Driever, W., and Fishman, M.C. (1996). Mutations affecting development of zebrafish digestive organs. Development *123*, 321–328. https://doi.org/10.1242/dev.123.1.321.

Pan, Y.A., Freundlich, T., Weissman, T.A., Schoppik, D., Wang, X.C., Zimmerman, S., Ciruna, B., Sanes, J.R., Lichtman, J.W., and Schier, A.F. (2013). Zebrabow: multispectral cell labeling for cell tracing and lineage analysis in zebrafish. Development *140*, 2835–2846. https://doi.org/10.1242/dev.094631.

Peron, M., Dinarello, A., Meneghetti, G., Martorano, L., Facchinello, N., Vettori, A., Licciardello, G., Tiso, N., and Argenton, F. (2020). The stem-like Stat3-responsive cells of zebrafish intestine are Wnt/β-catenin dependent. Development *147*, dev188987.

Ponder, B.A.J., Schmidt, G.H., Wilkinson, M.M., Wood, M.J., Monk, M., and Reid, A. (1985). Derivation of mouse intestinal crypts from single progenitor cells. Nature *313*, 689–691. https://doi.org/10.1038/313689a0.

Potten, C.S., Chwalinski, S., Swindell, R., and Palmer, M. (1982). The spatial organization of the hierarchical proliferative cells of the crypts of the small intestine into clusters of 'synchronized' cells. Cell Tissue Kinet. *15*, 351–370. https://doi.org/10.1111/j.1365-2184.1982.tb01053.x.

Powell, Anne E., Wang, Y., Li, Y., Poulin, Emily J., Means, Anna L., Washington, Mary K., Higginbotham, James N., Juchheim, A., Prasad, N., Levy, Shawn E., et al. (2012). The Pan-ErbB negative regulator Lrig1 is an intestinal stem cell marker that functions as a tumor suppressor. Cell *149*, 146–158. https://doi.org/10.1016/j.cell.2012.02.042.

Sakamori, R., Das, S., Yu, S., Feng, S., Stypulkowski, E., Guan, Y., Douard, V., Tang, W., Ferraris, R.P., Harada, A., et al. (2012). Cdc42 and Rab8a are critical for intestinal stem cell division, survival, and differentiation in mice. J. Clin. Invest. *122*, 1052–1065. https://doi.org/10.1172/jci60282.

Sangiorgi, E., and Capecchi, M.R. (2008). Bmi1 is expressed in vivo in intestinal stem cells. Nat. Genet. *40*, 915–920. https://doi.org/10.1038/ng.165.

Schmidt, G.H., Wilkinson, M.M., and Ponder, B.A. (1985). Cell migration pathway in the intestinal

epithelium: an in situ marker system using mouse aggregation chimeras. Cell *40*, 425–429. https://doi.org/10.1016/0092-8674(85)90156-4.

Snippert, H.J., Van Der Flier, L.G., Sato, T., Van Es, J.H., Van Den Born, M., Kroon-Veenboer, C., Barker, N., Klein, A.M., Van Rheenen, J., Simons, B.D., and Clevers, H. (2010). Intestinal crypt homeostasis results from neutral competition between symmetrically dividing Lgr5 stem cells. Cell *143*, 134–144. https://doi.org/10.1016/j.cell.2010.09.016.

Sumigray, K.D., Terwilliger, M., and Lechler, T. (2018). Morphogenesis and compartmentalization of the intestinal crypt. Dev. Cell *45*, 183–197.e5. https://doi.org/10.1016/j.devcel.2018.03.024.

Tsai, Y.-J., Pan, H., Hung, C.-M., Hou, P.-T., Li, Y.-C., Lee, Y.-J., Shen, Y.-T., Wu, T.-T., and Li, C. (2011). The predominant protein arginine methyltransferase PRMT1 is critical for zebrafish convergence and extension during gastrulation. FEBS J. *278*, 905–917. https://doi.org/10.1111/j.1742-4658.2011.08006.x.

Wallace, K.N., Akhter, S., Smith, E.M., Lorent, K., and Pack, M. (2005). Intestinal growth and differentiation in zebrafish. Mech. Dev. *122*, 157–173. https://doi.org/10.1016/j.mod.2004.10.009.

Wang, Z.Y., Du, J.G., Lam, S.H., Mathavan, S., Matsudaira, P., and Gong, Z.Y. (2010). Morphological and molecular evidence for functional organization along the rostrocaudal axis of the adult zebrafish intestine. BMC Genomics *11*, 392. https://doi.org/10.1186/1471-2164-11-392.

Warga, R.M., and Nusslein-Volhard, C. (1999). Origin and development of the zebrafish endoderm. Development *126*, 827–838. https://doi.org/10.1242/dev.126.4.827.

Westerfield, M. (2007). The Zebrafish Book. A Guide for the Laboratory Use of Zebrafish (Danio rerio) (University of Oregon Press).

Zhang, X., and Cheng, X. (2003). Structure of the predominant protein arginine methyltransferase PRMT1 and analysis of its binding to substrate peptides. Structure *11*, 509–520. https://doi.org/10.1016/s0969-2126(03)00071-6.

STAR★METHODS

KEY RESOURCES TABLE

REAGENT or RESOURCE	SOURCE	IDENTIFIER
Antibodies		
Rabbit anti-PRMT1 antibody	GeneTex	GTX128199
anti-β-actin antibody	ThermoFisher	PA1-46296; RRID:AB_2223196
Deposited Data		
Mendeley data	Source data	https://data.mendeley.com/datasets/zxhkgj2mnm/draft?a=b9a82eb1-285e-411b-9ed1-6d8186f47d33
Experimental models: Organisms/strains		
Zebrafish: *Tg* (*prmt1*:*mCherry-CreER*^{T2})	This Paper	N/A
Zebrafish: *ubi*:*Zebrabow*	Pan et al. (2013)	N/A
Oligonucleotides		
Primer: *prmt1* promoter (F:5′-GATGTTCA GAGGTGCAGGTTTGAC-3′, R: 5′-TTCGAT AAACTGGACACAGCCGCGAC-3′	This Paper	N/A
prmt1 MO (5′-TGTCTGCCGTCTCC GCCATTTCGAT-3′)	Gene Tools	ZFIN: ZDB-MRPHLNO-110629-2
Recombinant DNA		
Plasmid: *β-actin:mGFP*	Laboratory of V. Korzh (Institute of Molecular and Cell Biology (IMCB), Singapore)	N/A
Plasmid: *hsp70L:mCherry-CreER*^{T2}	Laboratory of S. Hans (Dresden University of Technology, Germany)	N/A
Plasmid: CreER^{T2}	Laboratory of N. Barker (IMCB, Singapore)	N/A
Software and algorithms		
ImageJ (v1.52t)	NIH	https://imagej.net/
Imaris (9.5.1)	Bitplane	https://imaris.oxinst.com
Huygens Professional (18.10.0)	Scientific Volume Imaging (SVI)	https://svi.nl/Huygens-Professional
MATLAB 2020b	MathWorks	https://es.mathworks.com/products/matlab.html
Prism® 8.3	GraphPad Software Inc., USA	https://www.graphpad.com/

RESOURCE AVAILABILITY

Lead contact

Further information and requests for resources, reagents and plasmids should be directed to and will be fulfilled by the lead contact, Sahar Tavakoli (sahartavakoli@fas.harvard.edu).

Material availability

Plasmids generated in this study are available from the lead contact with a completed Materials Transfer Agreement.

Data and code availability

Data

Raw, processed, and analyzed in this study are available for download from our Mendeley Data (https://data.mendeley.com/datasets/zxhkgj2mnm/draft?a=b9a82eb1-285e-411b-9ed1-6d8186f47d33).

Code
This paper does not report original code.

Any additional information required to reanalyze the data reported in this paper is available from the Lead contact upon request.

EXPERIMENTAL MODEL AND SUBJECT DETAILS

Fish and transgenic lines

All fish were bred and housed following standard zebrafish husbandry (Westerfield, 2007). In this study we used both male and female fish. The following transgenic line fish were used: *Tg* (*β-actin*:*mGFP*) and AB wild type for chimera generation (Figures 1A–1C), AB wild type for anti-PRMT1 antibody staining and EdU oral administration (Figure 2A and SF1), and *Tg* (*ubi*:*Zebrabow*) and *Tg* (*prmt1*:*mCherry-CreER*^{T2}) for lineage tracing experiments (Figures 2B, 3A, 3D–3G, S3, S4, S6, Videos S1,and S2).

Creation of chimera by cell transplantation

Donor cells from *Tg* (*β-actin*:*mGFP*) embryos (gift from V. Korzh) were transplanted into wild type host embryos. The dechorionated embryos were kept in Danieau solution at 28.5°C from 3 h postfertilization (blastula stage) to 6 h postfertilization (shield stage). Next, 25 donor cells from the presumptive intestine at the ventral margin were transplanted to the same position in host embryos. The chimeric embryos were transferred to Danieau solution and incubated at 28.5°C. Adult chimera zebrafish, three to five months old, were euthanized and intestinal sections were prepared for imaging.

Generation of transgenic lines of zebrafish for lineage tracing

To identify zebrafish ISC markers, first we screened the zebrafish genome for homologs of mouse or human ISC marker candidates documented in the literature (Matsuda and Shi, 2010; Sangiorgi and Capecchi, 2008; Powell et al., 2012) (Figure S2). We selected *prmt1*, which was reported in the simpler model organisms such as *C. elegans* (Zhang and Cheng, 2003) and suggested as a zebrafish ISC marker (Matsuda and Shi, 2010) for further analysis. *Tg* (*prmt1*:*mCherry-CreER*^{T2}) line was generated in-house as follows: the ISC promoter was amplified (F:5′-GATGTTCAGAGGTGCAGGTTTGAC-3′, R: 5′-TTCGATAAACTGGACACAG CCGCGAC-3′ amplicon size: 3494 bp), combined with the *mCherry-CreER*^{T2} fragment, and inserted between the Ds sites in the backbone pMDS6 plasmid. The final construct, *Tg* (*prmt1*:*mCherry-CreER*^{T2}), was co-injected with Ac mRNA to the 1–2 cell stage zebrafish embryos. The injected embryos were incubated at 28.5°C in E3 medium and grown to their adult stage under conventional conditions (Westerfield, 2007).

METHOD DETAILS

In vivo labeling of proliferating intestinal epithelium cells with EdU

Adult wild-type male zebrafish, close in age and weight (0.7 ± 0.05 g), were randomly chosen for the experiment and maintained as above. Prior to treatment, fish were anesthetized by gradual decrease in water temperature to 12°C. 10 μL of 10 mM EdU in 1X PBS was orally administrated to the anesthetized fish by gavaging the shortened microloader tip (Eppendorf) into the mouth and esophagus. EdU solution was delivered to the anterior portion of the foregut every 12 h and until the fish were euthanized (0.5–60 h after the first EdU pulse).

Morpholino oral administration

Vivo-Morpholinos (MOs) (Gene Tools, Philomath, OR) incorporate a knock-down sequence modified with a dendrimer delivery moiety. The *prmt1* MOs' sequence (5′-TGTCTGCCGTCTCCGCCATTTCGAT-3′) were published in previous studies (Tsai et al., 2011). The morpholino (MO) experiment was performed following the protocol published by Matsuda and Shi (2010). Briefly, 2 nmol (4 μL of 0.5 mM stock) of translation blocking *prmt1* Vivo-MO in PBS (PBS) was orally administrated to the anesthetized adult zebrafish by gavaging the shortened microloader tip (Eppendorf) into the mouth and esophagus. The *prmt1* Vivo-MO was administered once per day for 4 days and the intestinal tissue was harvested 2 days later (day 6).

QUANTIFICATION AND STATISTICAL ANALYSIS

All results are presented as raw data or mean ± SEM or min to max, where indicated. Statistical analysis was performed using the one-way ANOVA to test the Villus height in different groups. The correlation between

stripe width and the cell cluster length was measured using Graphpad Prism®; version 8.3. Sample size and treatment condition for each experiment are indicated in the figure legends. Results with p values of less than 0.05 were considered statistically significant: *p < 0.05; **p < 0.01; ***p < 0.001;; ****p < 0.0001; ns., not significant.

ADDITIONAL RESOURCES

Imaging

Tissue preparation for microscopy

All the tissue samples were from S2-S4 segments corresponding to the anterior and middle sections of the zebrafish intestine and feature gene expression profiles similar to the human small intestine (Wang et al., 2010).

For EdU labeling of proliferative cells, the adult zebrafish were euthanized at 0.5, 12, 24, 36, 48, and 60 h after the first EdU pulse. The dissected intestines were fixed in 4% paraformaldehyde, followed by cryoprotection embedding with 2% agarose and 5% sucrose and incubated in 30% sucrose solution at 4°C for overnight. The intact intestine specimen was embedded in tissue freezing medium (Leica 14020108926), rapidly frozen in liquid nitrogen and cross-sectioned with the cryostat at −25°C (Leica CM1850). The cross-sections were transferred to a room temperature Poly-L-lysine-coated slide followed by air-drying overnight. Sections were demembranated, decalcified, blocked and stained with 0.5% Triton X-100, 10 mM EGTA (pH 7.4), 3% BSA and click-iT EdU Alexa Fluor 488 (Invitrogen), respectively.

Chimeric intestines were prepared for immunofluorescence imaging by fixing the dissected intestines in 4% paraformaldehyde, followed by sectioning as above. Zebrabow recombinant intestines were prepared for immunofluorescence imaging by fixing the dissected intestines in 4% paraformaldehyde, followed by clearing (Erturk et al., 2012). Primary antibodies were used as follows: Rabbit anti-PRMT1 antibody (GTX128199) and anti-β-actin antibody (ThermoFisher PA1-46296). Secondary antibodies were from Tyramide-Alexa Fluor 647 (Invitrogen T20916) and Alexa Fluor 555 (Invitrogen A32727), respectively. The sections were protected by embedding in a mounting medium (Vectashield H-1400) and covered with a coverslip. The mounted slides were stored at 4°C in a light-protected condition to preserve the fluorescence before imaging.

Confocal microscopy

Images were acquired with either a Leica TCS SP5X (20×/0.70 and 40×/0.85 objectives) or a PerkinElmer UltraViewVoX Spinning Disk microscope (20×/0.60, 40×/1.15 and 60×/1.20 objectives). To measure the transit times of click-iT EdU-labeled cells, images were acquired with a Leica TCS SP5X with the laser line 405, 488, and 568. Other specimens were excited by laser wavelengths of 405, 433, 488, 514 and 568nm for DAPI, CFP, Alexa Fluor 488, YFP, and RFP, respectively.

Image processing and analysis

The images were deconvoluted with the theoretic point spread function generated from Huygens (18.10.0) and rendered in Imaris (9.5.1), ImageJ (v1.52t), and MATLAB (R2015a). For the EdU-labeled cell migration experiment, images from 25 cross-sections of 350–450 μm-tall villi for each treatment timepoint were selected and aligned. The signal intensity at each pixel were averaged over the 25 frames of each time point. Image processing for each timepoint were performed with the ImageJ software.

For the 3D reconstruction of recombinant VR/IVP segment, intensity normalization of the image stack was performed in MATLAB and 3D surface was generated in Imaris with surface smoothing parameter as 2.5 μm.

To quantify the size of an IVP cell cluster and its adjacent stripes, the intestine was rendered in 3D (Imaris, 9.5.1). Because the clusters are ellipsoidal with the major axis aligned along the intervillus pocket, we measured the lengths of the major (a) and minor axis (b) and reported the major axis as the cluster length. The width of the stripe was measured at mid-villus.